

Crystallization and Preliminary X-Ray Diffraction Analysis of BcOMT2 from *Bacillus cereus*: A Family of O-Methyltransferase

CHO, JANG-HEE¹, YOONGHO LIM², JOONG-HOON AHN², AND SANGKEE RHEE^{1*}

¹Department of Agricultural Biotechnology and Center for Agricultural Biomaterials, Seoul National University, Seoul 151-921, Korea

²Division of Bioscience and Biotechnology, Bio/Molecular Informatics Center, Konkuk University, Seoul 143-701, Korea

Received: October 13, 2006

Accepted: November 28, 2006

Abstract O-Methyltransferases (OMTs), one of the ubiquitous enzymes in plants, bacteria, and humans, catalyze a methyl-transfer reaction using S-adenosylmethionine and a wide range of phenolics as a methyl donor and acceptor, respectively. Substrates for most bacterial OMTs have largely remained elusive, but recent investigation using BcOMT2, an OMT from *Bacillus cereus*, suggested that *ortho*-dihydroxyflavonoids could serve as substrates. To elucidate the functional and structural features of BcOMT2, we expressed, and purified BcOMT2, and crystallized an apoenzyme and its ternary complex in the presence of a flavonoid and S-adenosylhomocysteine. Each crystal diffracted to 1.8 Å with its space group of *C*2 and *P*2₁2₁2₁, respectively. Structural analysis of apo-BcOMT2 and its ternary complex will provide the structural basis of methyl transfer onto (iso)flavonoids in a regiospecific manner.

Key words: *Bacillus cereus*, O-methyltransferase, crystallization

Members of the OMT family are a subset of methyltransferase that transfers the (a) methyl group to hydroxyl group(s) in substrate molecules in a regiospecific manner, resulting in the methylated products that have different cellular functions from those of substrates [2, 3]. The reaction has been observed to occur ubiquitously in many organisms, including bacteria, fungi, plants, and mammals. In general, OMTs exhibit two noticeable features. The enzymes have a highly conserved three-dimensional structure, an alternating β strands and α helices with some alterations at either N- or C-terminal regions [7]. In particular, structural and functional investigation for plant OMTs revealed distinctive structural variations and moreover two different, independent reaction mechanisms for lignin biosynthesis [1], and (iso)flavonoid

biosynthesis, respectively [12]. The second feature, which is a more significant characteristic of OMTs, resides in the diversity of substrate specificities, ranging from small molecules and lipids to macromolecules such as proteins, DNA, and RNA [7], although the natural substrates remain mostly unknown for bacterial OMTs. Because of these diversities, OMTs display relatively low sequence homology among members of the family, despite the conserved folding topology. Nonetheless, OMTs catalyze their reactions using an S-adenosylmethionine as a methyl donor, and subsequently form the methylated acceptor molecules and S-adenosylhomocysteine as products [10]. Recent investigation however showed several cases of exceptions in the overall structure of OMT; SET domain adopts a β -sheet topology (reviewed in [7]).

Given the presence of many putative OMTs in the bacterial genome sequences and their diverse substrate specificities, bacterial OMTs could serve as biocatalysts, in which the natural compounds, in particular phenolics, are modified on their hydroxyl groups in a position-specific way. Methylation of natural compounds using biocatalysts alters the chemical and physical properties of substrates, and has a wide range of implications in biotechnology [4, 5]. Recently, OMT from *Streptomyces coelicolor* A3(2) was shown to methylate *ortho*-dihydroxyflavones [11], and OMT from *Bacillus cereus* (BcOMT2) transfers a methyl group to the 3'- or 4'-hydroxyl group of flavonoids containing both 3'- and 4'-hydroxyl groups *in vitro* [6], although endogenous substrates of these two OMTs still remain elusive. These studies demonstrated that flavonoids could serve as exogenous substrates to these two bacterial OMTs, and further suggested that bacterial OMTs have a possible role in modulating exogenous compounds. In order to illuminate the structural and functional features of bacterial OMTs, we expressed, purified, and crystallized BcOMT2, and preliminary X-ray crystallographic analysis of BcOMT2 was carried out. The structural information

*Corresponding author

Phone: 82-2-880-4647; Fax: 82-2-873-3112;

E-mail: srheesnu@snu.ac.kr

gained from this study would provide insights of how bacterial OMT undergoes its reaction toward flavonoids.

For expression of BcOMT2, a 669-bp DNA fragment encoding an open reading frame for BcOMT2 [6] was generated by the polymerase chain reaction (PCR) with two primers (forward primer: 5'-ATCATATGAGTATGATTGAGACATGGACGGC-3'; reverse primer: 5'-ATGGATCCTCGTTATTCTTTTACGACTGCCAT-3') containing an NdeI site at the forward primer and a BamHI restriction enzyme site at the reverse primer. The PCR product was subcloned into the corresponding restriction sites of the modified pET28a plasmid vector (Novagen) including a tobacco etch virus (TEV) protease cleavage site. The resulting construct was transformed into *Escherichia coli* BL21(DE3) CodonPlus (Stratagene). The recombinant BcOMT2 protein contains five histidine residues and a TEV cleavage site at the N-terminus. The cells were grown at 37°C in 3 l of Luria-Bertani medium containing 50 µM kanamycin to an OD₆₀₀ of 0.75. The BcOMT2 was induced by adding isopropyl-thiogalactoside to the culture at the final concentration of 1 mM, and the culture was shaken for an additional 4 h at 37°C. Cells were harvested by centrifugation at 5,000 ×g for 10 min at 4°C. Harvested cells were resuspended in 80 ml of buffer A (20 mM NaH₂PO₄, 500 mM NaCl, 10 mM imidazole, pH 7.5) and 3 ml of sonication buffer containing 2 mg/ml lysozyme. Cells were shaken in an ice bath for 25 min and disrupted by sonication using 1–3-sec pulses at 225 W for 30 min with an ultrasonic processor (Cole-Parmer). The lysate was then centrifuged at 30,000 ×g for 50 min at 4°C, and the resulting supernatant was filtered through a 0.45-µm-pore-size filter. This filtrate was subsequently loaded onto a HiTrap Chelating HP column (Amersham Biosciences) charged with Ni²⁺, which is attached to a ÄKTA-fast protein liquid chromatography (FPLC) system (Amersham Biosciences). The column was washed extensively with 7 bed volumes of buffer A, and then eluted stepwise with increasing concentrations of imidazole in buffer B (20 mM NaH₂PO₄, 500 mM NaCl, 350 mM imidazole, pH 7.5). Eluted N-terminal His-tagged BcOMT2 was pooled based on SDS-PAGE analysis, and dialyzed against buffer C (50 mM Tris-HCl, pH 8.0). The His-tagged BcOMT2 was incubated with TEV protease (1.3 mg/ml) at 30°C for 4 h, and reloaded onto a HiTrap affinity column to purify the native BcOMT2, which is free of the His-tag. Finally, the enzyme was concentrated to ~8 mg/ml by Centricon (Millipore) against buffer C, and the SDS-PAGE analysis of BcOMT2 is shown in Fig. 1A. All purification procedures described here were performed at 4°C, and the recombinant BcOMT2 was purified to 11 mg per gram of cells. Molecular mass of the purified recombinant BcOMT2 was estimated to be about 26 kDa (Fig. 1A), and the enzyme appears to form a dimer in solution, based on results from Superdex 200 gel filtration chromatography (Fig. 1B). Since BcOMT2 exhibits relatively low sequence

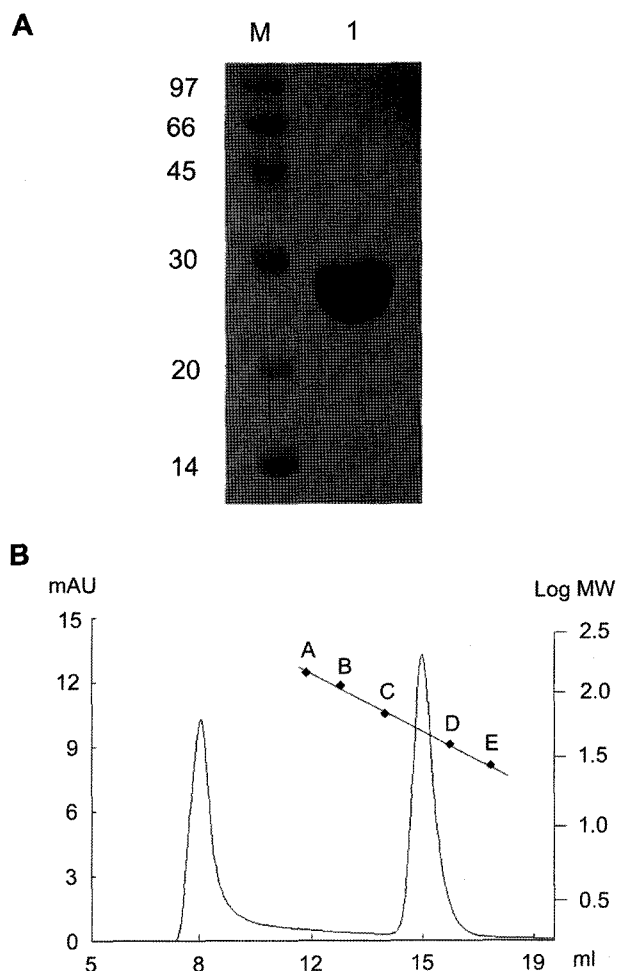


Fig. 1. SDS-PAGE and size-exclusion chromatographic analysis of the recombinant BcOMT2. **A.** Lane M, molecular weight markers (kDa); lane 1, the purified BcOMT2 after the removal of His-tag. **B.** Chromatogram by size-exclusion chromatography with standard molecular markers.

The first elution peak corresponds to that of Blue dextran, and the second peak is for 48 kDa, representing a homodimeric BcOMT2. The standard marker; A, β -amylase (200 kDa); B, alcohol dehydrogenase (150 kDa); C, albumin (66 kDa); D, carbonic anhydrase (29 kDa); E, cytochrome *c* (12.4 kDa).

homology with other OMTs whose structures were known, we prepared the selenomethionine (SeMet)-substituted protein. The plasmid harboring BcOMT2 was transformed into the methionine auxotroph *E. coli* B834(DE3) (Novagen), and the SeMet BcOMT2 was expressed and purified as described above.

Crystallization conditions were screened using the sitting-drop vapor-diffusion method by CrystalClear strips (Hampton Research) with Crystal screen I, II, Grid screen & PEG/ION (Hampton Research), and Wizard I & II (Emerald Biostructures). Typically, each drop was prepared by mixing 2 µl of the protein solution with 2 µl of the reservoir solution, and the plates were stored at 22°C. Native BcOMT2 protein tends to produce abnormal crystals

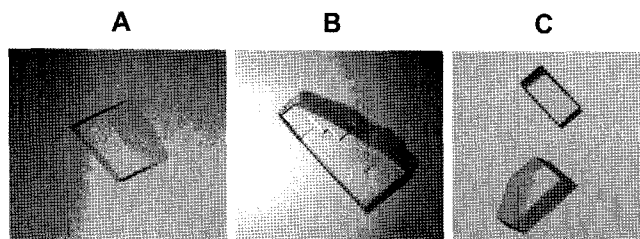


Fig. 2. Crystallization of the SeMet BcOMT2 protein. **A.** Crystal for apoenzyme was produced by using the SeMet BcOMT2. Addition of 3% dioxane was crucial in forming a well-formed single crystal. **B.** Ternary complex was crystallized, but these crystals were not usable owing to its multiplicity. **C.** Micro-seeding of BcOMT2 crystals in (**B**) as seeds resulted in single crystals for the ternary complex.

in the initial crystal screening, and therefore crystallization was carried out by using the purified SeMet BcOMT2 protein. Initially, apoenzyme (*i.e.*, in the absence of cofactor *S*-adenosylmethionine) was subjected to crystallization trials. After extensive search, crystals of apoenzyme were produced in a crystallization buffer of 0.1 M citric acid, pH 4.5, 1.0 M LiCl, 2% PEG 6000, plus 3% dioxane (Fig. 2A). Subsequently, a ternary complex of BcOMT2 with a putative substrate, 6,7-dihydroxyflavone, and a cofactor product, *S*-adenosylhomocysteine, was co-crystallized. Specifically, the SeMet BcOMT2 protein was first incubated with 2 mM 6,7-dihydroxyflavone, and crystals of the ternary complex were then grown in a buffer of 0.1 M citric acid, pH 5.2, 0.25 M LiCl, 20% PEG 6000, 1 mM *S*-adenosylhomocysteine, 2 mM MgCl₂, and 3% dioxane. However, those preliminary crystals were not suitable for data collection (Fig. 2B), and after extensive manipulation of those crystals by micro-seeding, a well-formed single crystal was produced (Fig. 2C).

For diffraction studies, crystals of apoenzyme and its ternary complex were soaked shortly in a cryoprotectant

solution, which was the crystallization solution plus 25% glycerol, respectively. Each crystal diffracted to 1.8 or 1.6 Å using the synchrotron radiation on beamline 4A MXW at the Pohang Accelerator Laboratory (Pohang, Korea). The images were indexed and scaled using HKL2000 [9]. Table 1 lists the relevant statistics of data for apoenzyme and the ternary complex collected at 4A beamline. Two crystals belonged to a different space group, but the calculated crystal volume per protein mass (V_M) suggested that there are two monomers in an asymmetric unit [8], consistent with a homodimer of BcOMT2 in solution (Fig. 1B). The structure determination of BcOMT2 is currently under way, and the structural analysis of apo-BcOMT2 and its ternary complex will provide a structural basis of methyl transfer onto (iso)flavonoids in a regiospecific manner.

Acknowledgment

This work was supported by a Korea Research Foundation Grant (KRF-2003-041-F00017), Republic of Korea.

REFERENCES

- Ferrer, J.-L., C. Zubieta, R. A. Dixon, and J. P. Noel. 2005. Crystal structures of alfalfa caffeoyl coenzyme A 3-O-methyltransferase. *Plant Physiol.* **137**: 1009–1017.
- Hahlbrock, K. and D. Scheel. 1989. Physiology and molecular biology of phenylpropanoid metabolism. *Annu. Rev. Plant Physiol. Plant Mol. Biol.* **40**: 347–369.
- Khosla, C. 2000. Natural product biosynthesis: A new interface between enzymology and medicine. *J. Org. Chem.* **65**: 8127–8133.

Table 1. Data collection statistics of SeMet BcOMT2 crystals.

	Apoenzyme	Ternary complex
Space group	C2	$P2_12_12_1$
Wavelength (Å)	0.97929	0.97928
Cell dimension (Å)	a=124.9, b=64.4, c=86.3 Å $\alpha, \gamma=90, \beta=133.7^\circ$	a=66.6, b=74.2, c=90.7 Å $\alpha, \beta \gamma=90^\circ$
Resolution range (Å)	50.0–1.8 (1.86–1.80)	50.0–1.60 (1.66–1.60)
Observed reflections	331,448	818,655
Unique reflections	45,855 (4,505)	57,762 (3,975)
Redundancy	7.2 (7.2)	14.2 (12.9)
Completeness (%)	99.9	95.7
R_{sym} (%)	7.2 (35.9)	13.5 (20.0)
$I/\sigma(I)$	30.8 (4.4)	25.7 (12.1)
No. molecules in AU	2	2
V_m (Å ³ /Da)	2.65	2.27

Values for the last shell are in parentheses.

$R_{sym} = \sum_{hkl} |I_{hi} - \langle I_{hi} \rangle| / \sum_{hkl} I_{hi}$, where h denotes hkl and i counts through all symmetry-related reflections.

4. Kim, H.-A., D.-Y. Yoon, S.-M. Lee, S.-H. Baek, G.-H. Han, Y.-H. Kho, and C.-H. Lee. 2005. Screening and biotransformation of interleukin-1 β converting enzyme production inhibitors from *Arctii fructus*. *J. Microbiol. Biotechnol.* **15**: 269–273.
5. Kim, Y. M., K. Park, J.-H. Choi, J.-E. Kim, and I.-K. Rhee. 2004. Biotransformation of the fungicide chlorothalonil by bacterial glutathione S-transferase. *J. Microbiol. Biotechnol.* **14**: 938–943.
6. Lee, H. J., B. G. Kim, and J.-H. Ahn. 2006. Molecular cloning and characterization of *Bacillus cereus* O-methyltransferase. *J. Microbiol. Biotechnol.* **16**: 619–622.
7. Martin, J. L. and F. M. McMillan. 2002. SAM (dependent) I AM: The S-adenosylmethionine-dependent methyltransferase fold. *Curr. Opin. Struct. Biol.* **12**: 783–793.
8. Matthews, B. W. 1968. Solvent content of protein crystals. *J. Mol. Biol.* **33**: 491–497.
9. Otwinowski, Z. and W. Minor. 1997. Processing of X-ray diffraction data collected in oscillation mode. *Methods Enzymol.* **276**: 307–326.
10. Schubert, H. L., R. M. Blumenthal, and X. Cheng. 2003. Many paths to methyltransfer: A chronicle of convergence. *Trends Biochem. Sci.* **28**: 329–335.
11. Yoon, Y., Y. S. Yi, Y. Lee, S. Kim, B. G. Kim, J.-H. Ahn, and Y. Lim. 2005. Characterization of O-methyltransferase ScOMT1 cloned from *Streptomyces coelicolor* A3(2). *Biochim. Biophys. Acta* **1730**: 85–95.
12. Zubieta, C., X.-Z. He, R. A. Dixon, and J. P. Noel. 2001. Structures of two natural product methyltransferases reveal the basis for substrate specificity in plant O-methyltransferases. *Nat. Struct. Biol.* **8**: 271–279.